Progress In Electromagnetics Research Letters, Vol. 52, 1–9, 2015

An Open-Sleeve Folded U-Shaped Multiband Antenna

Elodie Georget[1, 2, *], Redha Abdeddaim[1], Franck Garde[3], and Pierre Sabouroux[1]

Abstract—In this paper, a multiband flexible antenna is presented. This antenna was realized on a flexible substrate in order to realize a deployable system for a distress beacon. We used the concept of open-sleeve antenna to change a quadrupole mode into a dipole mode. The main radiating element of the antenna is a dual-band folded U-shaped antenna. The operating frequencies of this antenna are studied depending on the length of the parasitic elements. In order to understand the matching and the radiation patterns in far field of both antennas (U-shaped and open-sleeve), their magnetic behaviors in near field are studied in simulation and in measurement. The simulated and measured radiation patterns are also presented to check the study in near field.

1. INTRODUCTION

The objective of the BELOCOPA project is the development of an autonomous, embedded and removable beacon to localize and collect the data of a crashed plane in sea. Our objective was to realize a deployable multiband antenna for this distress beacon. This antenna has to be flexible and has to radiate dipole modes at three resonance frequencies in the UHF band.

These last years, a lot of radio-communication embedded systems, very small and flexible antennas have been developed [1–7]. Some antennas for example can be integrated in an inflatable system, like in a sonobuoy [8], or in a lifejacket [9, 10].

In order to realize a multiband antenna, different techniques can be used, like associating monopoles [11], designing a fractal antenna [12] or a wideband antenna [13]. In this paper, we present a new design of dipolar multiband antenna. This design is based on the concept of open-sleeve antenna associated with dual-band systems. Previous papers [14, 15] shown that an open-sleeve monopole antenna is equivalent to a dual-band antenna with dipole modes thanks to parasitic elements. So as to obtain a tri-band antenna with dipole modes, we use the principle of the open-sleeve antenna on an antenna that radiates naturally two dipole modes by changing the quadrupole mode into a dipole mode with parasitic elements. The main element of our antenna is a folded U-shaped antenna that radiates two dipole modes. Adding parasitic elements, we change the third mode which is quadrupole into a dipole mode. This antenna is studied with and without the parasitic elements. Both configurations are studied in near field and in far field. The simulation results presented in this paper are done with the transient solver of the software CST Microwave Studio.

2. ANTENNA DESIGN

The antenna is realized on a surface $W_0 \times L_0 = 50\,\text{mm} \times 250\,\text{mm}$. This antenna is called folded U-shaped antenna because it looks like a capital letter "U" with its arms folded inside the "U" (Figure 1). The folded U-shaped antenna is represented on Figure 1(b) and the realized open-sleeve folded U-shaped antenna is represented on Figure 1(c).

Received 16 December 2014, Accepted 5 February 2015, Scheduled 4 March 2015

* Corresponding author: Elodie Georget (elodie.georget@cea.fr).

[1] Aix Marseille Université, CNRS, Centrale Marseille, Institut Fresnel, UMR 7249, Campus Universitaire de Saint Jérôme, Marseille 13013, France. [2] CEA-Saclay, DSV/I2BM/Neurospin, Gif-sur-Yvette Cedex 91191, France. [3] Tethys, Parc d'Activités de Signes, Avenue de Madrid, Signes 83870, France.

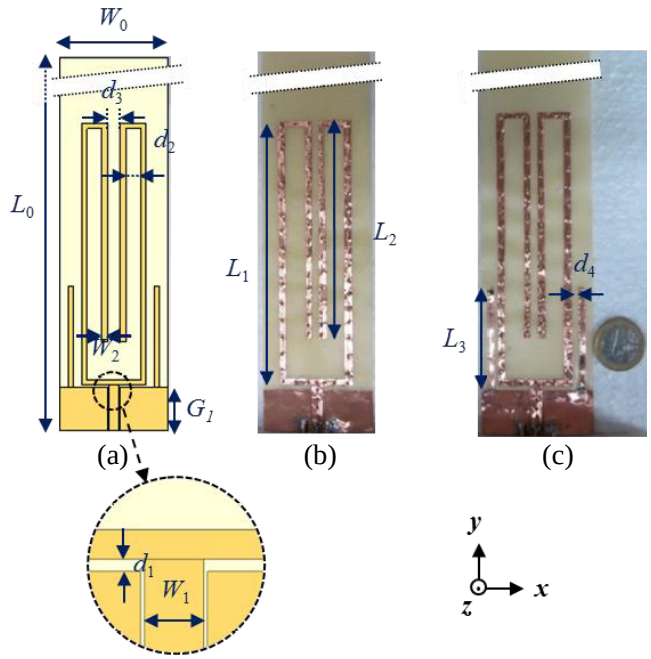

Figure 1. (a) Geometry of the open-sleeve folded U-shaped antenna. Realization of the folded U-shaped antenna (b) without and (c) with the parasitic elements. Dimensions in mm: $L_0 = 250$; $L_1 = 120$; $L_2 = 100$; $L_3 = 46$; $W_0 = 50$; $W_1 = 5$; $W_2 = 2.5$; $d_1 = 1$; $d_2 = 6$; $d_3 = 7$; $d_4 = 3.75$; $G_1 = 20$. A part of the top of the substrate of antenna is cut (represented by two discontinuous black lines in diagonal) because the substrate height is too long to visualize correctly the form of the antenna.

The flexible substrate of the antenna is made by polyurethane coated polyester material, with 0.32 mm thickness and a relative permittivity $\varepsilon_r^* = (3.0 - j0.2)$. This permittivity is retrieved using transmission/reflection method in a coaxial line [16, 17]. The metallic parts are realized with 35 µm thickness copper tape. To consolidate the main radiated element, the folded U-shaped part is hand sewn on the substrate with a metallic wire (0.02 mm in diameter). This hand sewing on the flexible substrate induces some ripples along the folded U-shaped part that are difficult to design in simulation. The feeding of the antenna is a coplanar line with 50 Ω characteristic impedance. The dimensions of the ground plane are $W_0 = 50$ mm and $G_1 = 20$ mm.

The two parasitic elements with length $L_3 = 46$ mm and width W_2 are added to the folded U-shaped antenna at a distance $d_4 = 3.75$ mm from the outer of the U-shaped.

3. FOLDED U-SHAPED ANTENNA

3.1. Resonance Frequencies

The reflection coefficient S_{11} of the folded U-shaped antenna was measured in an anechoic chamber on the frequency band [300–2300] MHz. In Figure 2, the simulated and measured reflection coefficients are represented in continuous and discontinuous line respectively. The measured S_{11} coefficient does not match the simulated S_{11} coefficient perfectly because the sewing of the U-shaped part of the antenna causes some geometric distortions not taken into account in the simulation. Nevertheless, the simulated and measured results are in agreement, we can note four resonant modes. The first mode is located at the frequency $f_1 = 590$ MHz, this frequency is done by length $L_A = (L_1 + d_2) = \lambda_1/4$, with λ_i the wavelength of the ith mode. The second mode is at $f_2 = 875$ MHz corresponding to the length $L_B = L_2 - d_2 = 1.1(\lambda_2/4)$. The second mode is better matched in measurement than in simulation. The two other resonance frequencies, $f_3 = 2.8 \times f_1 = 1670$ MHz and $f_4 = 2.5 \times f_2 = 2150$ MHz, correspond to the quadrupole modes generated by the length L_A and L_B respectively. The behavior of this antenna can be approximated by the combination of two uncoupled dipoles with lengths L_A and L_B.

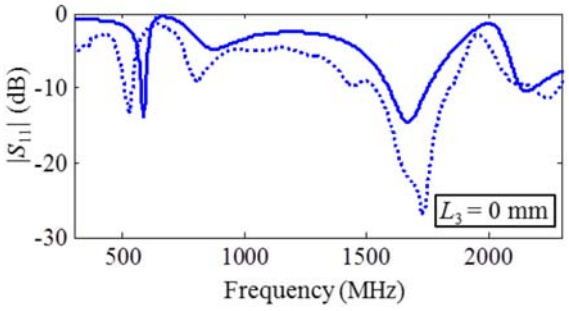

Figure 2. Reflection coefficient $|S_{11}|$ (dB) of the folded U-shaped in simulation (continuous line) and in measurement (discontinuous line).

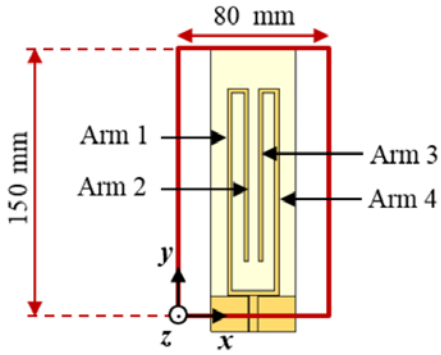

Figure 3. Scanned surface in near field of the folded U-shaped antenna.

3.2. Near Field Results

To understand the behavior of the antenna in far field, the magnetic field is studied. Indeed, the current distribution along the radiating elements of the antenna provides a complete description of the radiation pattern. To do this, we developed an experimental setup to measure the magnetic field at a studied point $\overrightarrow{H(x)}$ above the antenna since it is directly proportional to the current distribution in the studied space $\overrightarrow{J(x')}$ [18]:

$$\overrightarrow{H(x)} = \frac{1}{\mu_0}\nabla \times \left(\frac{\mu_0}{4\pi} \int \overrightarrow{J(x')} \frac{e^{ik|x-x'|}}{|x-x'|} d^3x' \right) \tag{1}$$

μ_0 the permeability of free space, k the wavenumber, x the studied point and x' a point in the studied space. For the configuration of our antenna, only H_x and H_z participate to the radiations. The H_x component has a vertical symmetry, and the H_z component has vertical and horizontal symmetry. Because our antennas are geometrically symmetric on the vertical axis, the H_x component is sufficient to describe the nature of the studied mode. We plot the real part of the field, because it gives information on the amplitude and phase of H_x. The measurement is realized in an anechoic chamber thanks to a 3D axis positioning system. The probe is a magnetic loop with $d = 5\,\text{mm}$ diameter ($d < (0.03\lambda_i)$, $i = \{1, 2, 3\}$). The probe is positioned 7 mm above the antenna ($7\,\text{mm} < 0.04\lambda_i$). The magnetic field is measured on a surface delimited by the red rectangular in Figure 3.

The normalized real part of H_x is visualized in Figure 4 for the folded U-shaped antenna without parasitic elements in simulation and measurement. The magnetic field H_x is represented at the three resonance frequencies f_1, f_2 and f_3. The simulated and measured results are in good agreement. Figures 4(a) and 4(b) represent the real part of H_x of the folded U-shaped antenna, at the first mode f_1 in simulation and measurement respectively. The magnetic field along the antenna has a positive sign inside the arms of folded U-shaped antenna (arm 2, arm 3), and it has a negative sign on the outer arms (arm 1, arm 4) of the folded U-shaped. The direction of the current is represented with white arrows in Figure 4(a). Then, the direction of the current is anti-clockwise (if the arms 2 and 3 are spread, the current moves in the same direction).

The real part of H_x at the second mode of the antenna is represented in Figure 4(c) (simulation) and 4(d) (measurement). The way of the current is in the same direction on the inner arms 2 and 3 (positive sign), and has two opposite directions (negative and positive signs) on the outer arms 1 and 4 of the antenna. The resulting electromagnetic mode is dipolar [15]. Effectively, the dominant current moves in a single direction, on the inferior part of the outer arms 1 and 4, and then on the inner arms 2 and 3 of the antenna.

Figures 4(e) and 4(f) represent the real part of H_x of the folded U-shaped antenna at the third mode f_3. Two distinct areas are noticeable, $\text{Re}(H_x)$ of the upper part of the antenna has negative sign and $\text{Re}(H_x)$ of the lower part has positive sign. The magnetic field is in phase opposition on the superior and inferior arms of the antenna. This third mode is then quadrupole.

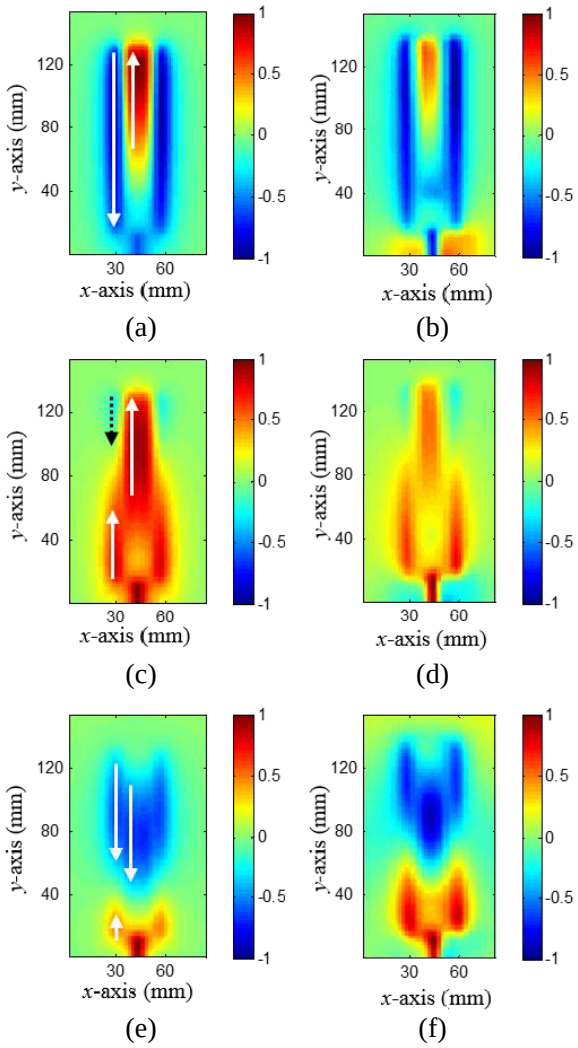

Figure 4. Normalized Re(H_x) map of the folded U-shaped antenna at f_1 in (a) simulation and (b) measurement, at f_2 in (c) simulation and (d) measurement, and at f_3 in (e) simulation and (f) measurement. The arrows show the direction of the current on the left half of the antenna.

3.3. Far Field Results

The radiation patterns of the folded U-shaped antenna are represented on Figure 5 for the three first resonance frequencies. The radiations are visualized in three dimensions thanks to the simulation results. The radiation patterns are measured in the anechoic chamber of *Centre Commun de Ressources en Microondes* (*C.C.R.M., Marseille, France*). The distance between the antenna under test and the receiver antenna is 8.40 m [14]. The antenna is positioned vertically at the center of the polar coordinates. The top of the antenna is at $\theta = 0°$, and the ground plane is at $\theta = +/-180°$.

The differences between simulation and experiment results are due to the geometric differences between the designed and realized antenna. Indeed, the distortions induced with the sewing of the U-shaped part on the flexible substrate are not simulated. For the two first resonance frequencies f_1 and f_2 (Figures 5(a)–(d)), the radiation patterns are actually dipolar in simulation and measurement. The gains in simulation are similar for f_1 (1.34 dB) and f_2 (1.39 dB). At the third resonance frequency f_3 (Figures 5(e)–(f)), the radiation patterns in simulation and measurement are quadripolar, as expected from the conclusions in near field. The quadripolar patterns are asymmetric due to the ground plane (smaller lobes in the inferior part). The differences of amplitude of the two inferior lobes between the

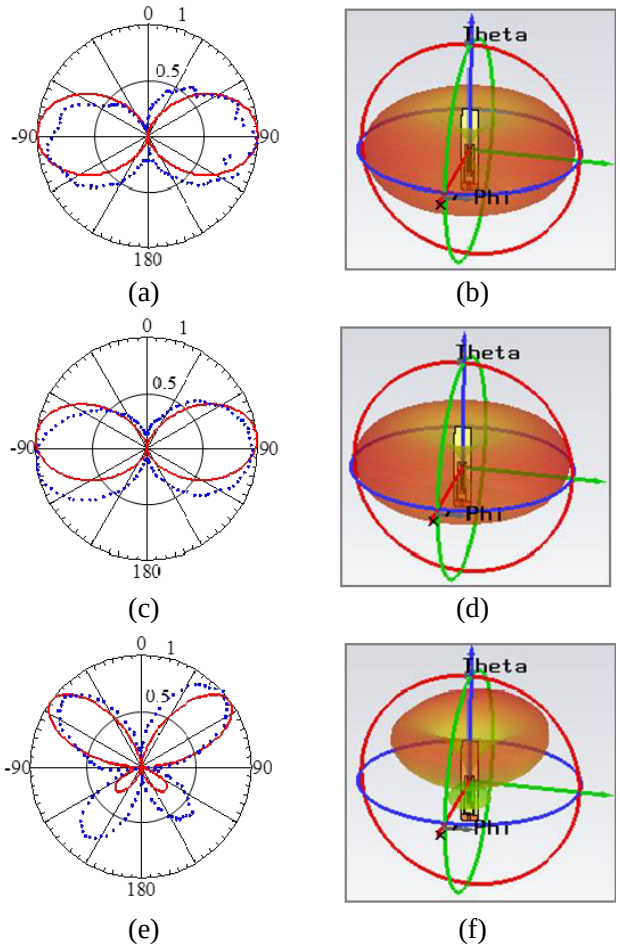

Figure 5. Folded U-shaped antenna. Normalized radiation pattern in linear in the E-plane, in simulation (continuous red line) and in measurement (blue points) at the frequencies (a) f_1, (c) f_2, and (e) f_3. Simulated radiation pattern in three dimensions at the frequencies (b) f_1, (d) f_2, and (f) f_3.

simulated and measured results are due to the connector position. The feeding connector of the antenna is in this plane in measurement. The gain of the folded U-shaped antenna at f_3 is 1.77 dB in simulation.

4. OPEN-SLEEVE FOLDED U-SHAPED ANTENNA

The aim is to get dipole modes at the first three resonance frequencies.

4.1. Resonance Frequencies

In order to choose the length L_3 of the parasitic elements to obtain a multiband antenna, the matching of the antenna depending on the length L_3 is studied in simulation. The reflection coefficient $|S_{11}|$ in dB on the frequency band [300–2300] MHz is represented in Figure 6 according to the length L_3. The 10 dB impedance bandwidths ($|S_{11}| < -10$ dB) are represented in light blue or dark blue. The case of the folded U-shaped antenna without parasitic element is framed for $L_3 = 0$ mm on Figure 6 (at the bottom of the figure).

Figure 6 shows that length L_3 of the parasitic elements does not have the same effect on the modes of the folded U-shaped antenna. The frequency position of the first mode (590 MHz) is not affected by the parasitic elements up to they reach the length $L_3 = 75$ mm. The first mode is extinct from

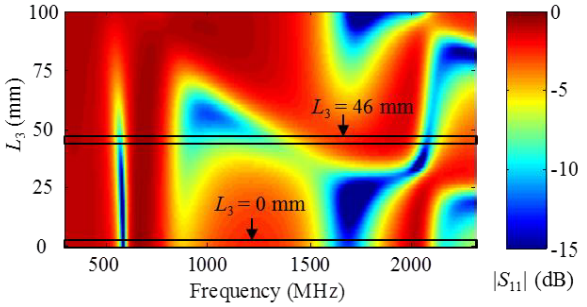

Figure 6. Reflection coefficient $|S_{11}|$ (dB) of the folded U-shaped antenna on the frequency band [300–2300] MHz depending on the length of the parasitic elements L_3.

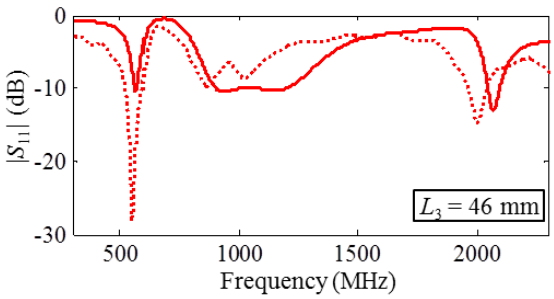

Figure 7. Reflection coefficient $|S_{11}|$ (dB) of the open-sleeve folded U-shaped antenna in simulation (continuous line) and in measurement (discontinuous line).

this length, this gives the maximum length of the parasitic elements ($L_3 = 75$ mm). The frequency position of the second resonance frequency is few affected by the parasitic elements up to they reach $L_3 = 75$ mm. The second mode is also extinct at the length $L_3 = 75$ mm. However, the matching of the second mode is better with the parasitic elements. For the third mode, the resonance frequency is very affected by the length L_3. When the parasitic elements are longer, the third mode resonates in a lower frequency. From $L_3 = 40$ mm, the resonance frequency of the second and third modes are close to constitute a wideband mode.

With this configuration, a dual-band antenna is obtained with a narrow band dipole mode and a second wideband mode, assumed dipole. In order to validate our supposition, the length of the parasitic elements was chosen $L_3 = 46$ mm (framed in the middle on Figure 6). The folded U-shaped antenna with parasitic elements of length $L_3 = 46$ mm is called the open-sleeve folded U-shaped antenna. Figure 7 shows the reflection coefficients in simulation and in measurement of this antenna. The first mode in simulation and in measurement is at the frequency $f_1' = 550$ MHz. In simulation, the second mode is a wideband mode as explained previously. In measurement, some differences appear. However, the third mode is lower in frequency compared to the third mode the folded U-shaped antenna without parasitic elements. The second and third mode in measurement are at the frequencies $f_2' = 850$ MHz and $f_3' = 1010$ MHz respectively.

4.2. Near Field Results

Figure 8 shows the normalized real part of H_x of the open-sleeve folded U-shaped antenna with parasitic elements ($L_3 = 46$ mm), in simulation and measurement at the three resonance frequencies f_1', f_2' and f_3'. The results in simulation and measurement are in good agreement. Figures 8(a) and 8(b) represent the real part of H_x at the first mode f_1' of the open-sleeve folded U-shaped antenna.

The magnetic field is in phase opposition on the inner and outer tracks of the antenna, so the parasitic elements do not alter the first dipole mode.

The real part of H_x at the second mode of the open-sleeve antenna is represented in Figure 8(c) in simulation and 8(d) in measurement. The magnetic field has a dipolar behavior on the inner tracks, and a quadripolar behavior on the outer tracks of the folded U-shaped. As for the parasitic elements, they have a dipolar behavior in phase opposition to the inner tracks. This mode at f_2' keeps the dipolar behavior, the adding of the parasitic elements behaves like a matching circuit.

Figures 8(e) and 8(f) represent the real part of H_x of the open-sleeve antenna at the third mode f_3'. The magnetic field has still a quadripolar behavior on the folded U-shape of the open-sleeve antenna. Along the folded U-shaped, the two parts positive and negative of Re(H_x) on Figure 4(f) have opposite signs to the two parts of Re(H_x) of the quadrupole mode of the folded U-shaped antenna (Figures 4(e) and 4(f)). This difference is explained by the different position of the third resonance frequency of the antenna with and without the parasitic elements. The parasitic elements have a dipolar behavior, and the inferior part of the quadrupole mode is bypassed. This mode presents a dipole mode, like the case of the open-sleeve monopole antenna [15].

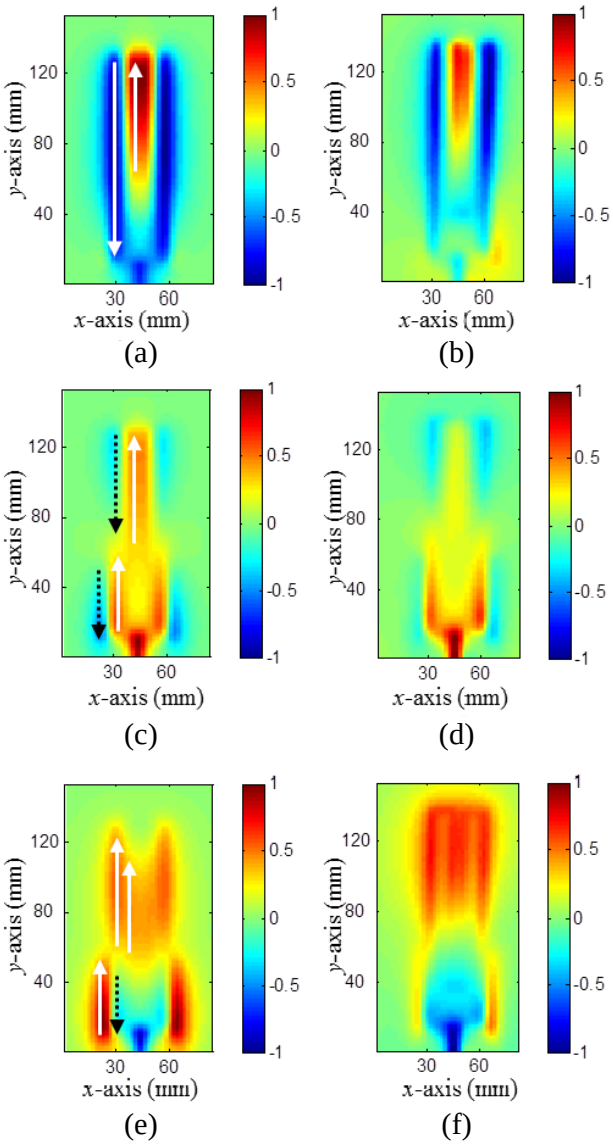

Figure 8. Normalized Re(H_x) map of the open-sleeve folded U-shaped antenna ($L_3 = 46$ mm) at f_1' in (a) simulation and (b) measurement, at f_2' in (c) simulation and (d) measurement, and at f_3' in (e) simulation and (f) measurement. The arrows show the direction of the current on the left half of the antenna.

4.3. Far Field Results

When the parasitic elements are added to the folded U-shaped antenna, the three radiation patterns on Figure 9 are obtained. In the same way as the radiation patterns of the folded U-shaped antenna (Figure 5), some differences between simulation and measurement result are due to the difficulty to simulate the realized antenna with the ripples of the sewing. The radiation patterns at the three first resonance frequencies are dipolar in simulation and in measurement.

In simulation, the gains of the open-sleeve folded U-shaped antenna are 1.35 dB at the first resonance frequency f_1', 1.42 dB at the second resonance frequency f_2' and 1.47 dB at the third resonance frequency f_3'.

The quadrupole mode of the folded U-shaped antenna has been changed into a dipole mode adding parasitic elements that resonate at the third mode.

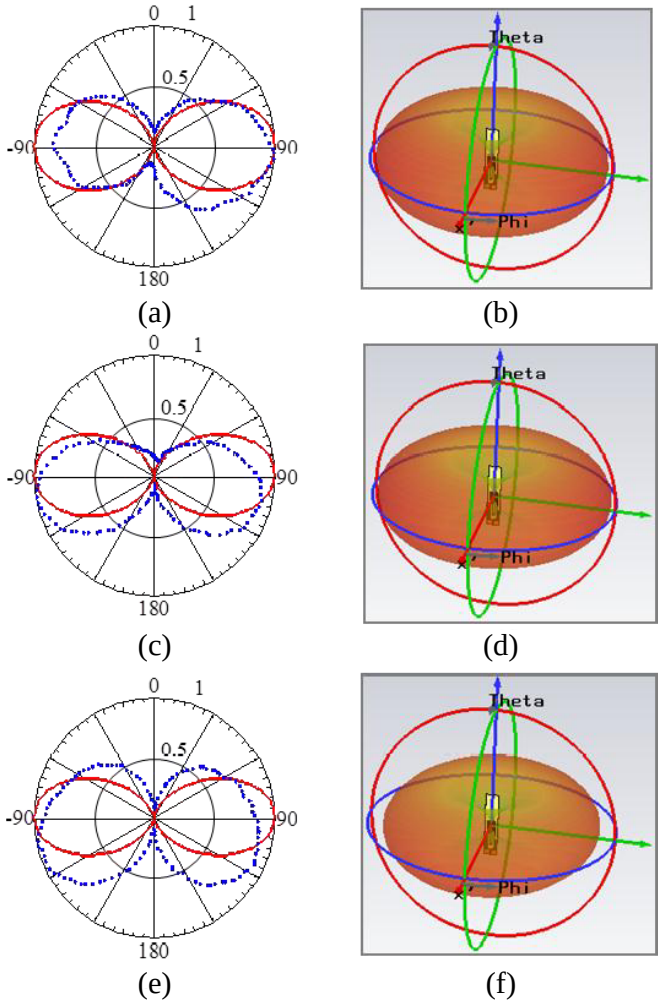

Figure 9. Open-sleeve folded U-shaped antenna ($L_3 = 46\,\text{mm}$). Normalized radiation pattern in linear, in the E-plane in simulation (continuous red line) and in measurement (blue points) at the frequencies (a) f_1', (c) f_2', and (e) f_3'. Simulated radiation pattern in three dimensions at the frequencies (b) f_1', (d) f_2', and (f) f_3'.

5. CONCLUSION

With the study of this folded U-shaped antenna, we are able to realize a multiband antenna thanks to the adding of the parasitic elements. Two modes of this antenna can be tuned modifying the dimensions of the folded U-shaped antenna whereas the third mode is generated through the parasitic elements. The advantage of this antenna is the matching in term of resonance frequency for the third mode. Indeed, we can obtain a tri-band antenna or a dual-band wideband antenna depending on the parasitic elements length.

The aim of this work is to realize an ejected maritime beacon during an aircraft crash in the sea (BELOCOPA project). Initially, the antenna was studied in free space.

ACKNOWLEDGMENT

This work was supported by the French Fonds Unique Interministériel, with the support of the Provence Alpes Côte d'Azur Region and Bpifrance in the context of the BELOCOPA project. Redha Abdeddaim is thankful for a PEPS CNRS funding through project CLOAK EXTERNE.

REFERENCES

1. De Cos, M. E. and F. Las-Heras, "Polypropylene-based dual-band CPW-fed monopole antenna," *IEEE Antennas Propag. Mag.*, Vol. 55, No. 3, 264–273, Jun. 2013.
2. Paul, D. L., L. Zhang, and L. Zheng, "Flexible dual-band LCP antenna for RFID applications," *Proc. IEEE EMTS*, 973–976, Hiroshima, Japan, May 2013.
3. Salam, A., A. Khan, and M. S. Hussain, "Dual band microstrip antenna for wearable applications," *Microw. Opt. Technol. Lett.*, Vol. 56, No. 4, 916–918, Apr. 2014.
4. Wang, Z., L. Z. Lee, D. Psychoudakis, and J. Volakis, "Embroidered multiband body-worn antenna for GSM/PCS/WLAN communications," *IEEE Trans. Antennas Propag.*, Vol. 62, No. 6, 3321–3329, Jun. 2014.
5. Khaleel, H. R., H. M. Al-Rizzo, and D. G. Rucker, "Compact polyimide-based antennas for flexible displays," *IEEE Journal of Display Technology*, Vol. 8, No. 2, 91–97, Feb. 2012.
6. Abbosh, A. I., R. F. Babiceanu, H. Al-Rizzo, S. Abushamleh, and H. R. Khaleel, "Flexible Yagi-Uda antenna for wearable electronic devices," *APSURSI IEEE*, 1200–1201, Orlando, FL, USA, Jul. 2013.
7. Raad, H. R., A. I. Abbosh, H. M. Al-Rizzo, and D. G. Rucker, "Flexible and compact AMC based antenna for telemedicine applications," *IEEE Trans. Antennas Propag.*, Vol. 61, No. 2, 524–531, Feb. 2013.
8. Min, K.-S., Y.-H. Park, and K.-W. Im, "Design for sonobuoy transmitting antenna for anti-submarine warfare," *Proc. IEEE Antennas Propag. Int. Symp.*, 1201–1204, Sendai, Japan, Aug. 2004.
9. Serra, A. A., P. Nepa, and G. Manara, "A wearable two-antenna system on a life jacket for Cospas-Sarsat personal locator beacons," *IEEE Trans. Antennas Propag.*, Vol. 60, No. 2, 1035–1042, Feb. 2012.
10. Lilja, J., et al., "Body-worn antennas making a splash: Lifejacket-integrated antennas for global search and rescue satellite system," *IEEE Antennas Propag. Mag.*, Vol. 55, No. 2, 324–341, Apr. 2013.
11. Chu, Q.-X. and L.-H. Ye, "Design of compact dual-wideband antenna with assembled monopoles," *IEEE Trans. Antennas Propag.*, Vol. 58, No. 12, 4063–4066, Dec. 2010.
12. Li, D. and J. Mao, "Sierpinskized Koch-like sided multifractal dipole antenna," *Progress In Electromagnetics Research*, Vol. 130, 207–224, 2012.
13. Durgun, A. C., C. A. Balanis, C. R. Birtcher, and D. R. Allee, "Design, simulation, fabrication and testing of flexible bow-tie antennas," *Proc. IEEE Radio and Wireless Symp.*, 50–53, Phoenix, AZ, USA, Jan. 2011.
14. Georget, E., R. Abdeddaim, and P. Sabouroux, "Analytical, simulation and measurement studies of a dual-band open-sleeve curved meander line antenna on a flexible substrate," *Progress In Electromagnetics Research*, Vol. 145, 49–57, 2014.
15. Georget, E., R. Abdeddaim, and P. Sabouroux, "AMTA corner: A new method to design a multi-band flexible textile antenna," *IEEE Antennas Propag. Mag.*, Vol. 56, No. 3, 240–248, Jun. 2014.
16. Nicolson, M. and G. F. Ross, "Measurement of the intrinsic properties of materials by time-domain techniques," *IEEE Trans. Intrum. Meas.*, Vol. 19, No. 4, 377–382, Nov. 1970.
17. Georget, E., R. Abdeddaim, and P. Sabouroux, "A quasi-universal method to measure the electromagnetic characteristics of usual materials in the microwave range," *Comptes Rendus — Physique*, Vol. 15, No. 5, 448–457, May 2014.
18. Jackson, J. D., "Radiating systems, multipole fields and radiation," *Classical Electrodynamics*, 3rd edition, 407–455, Wiley, New York, 1962.